

## A 76.5-92.6 GHz CMOS LNA Using Two-Port kQ-Product Theory for Transformer Design

Zhang, Youming; Wei, Zhennan; Tang, Xusheng; Zhang, Linghan; Huang, Fengyi

**DOI**

[10.1109/LMWC.2022.3170929](https://doi.org/10.1109/LMWC.2022.3170929)

**Publication date**

2022

**Document Version**

Final published version

**Published in**

IEEE Microwave and Wireless Components Letters

**Citation (APA)**

Zhang, Y., Wei, Z., Tang, X., Zhang, L., & Huang, F. (2022). A 76.5-92.6 GHz CMOS LNA Using Two-Port kQ-Product Theory for Transformer Design. *IEEE Microwave and Wireless Components Letters*, 32(10), 1187-1190. <https://doi.org/10.1109/LMWC.2022.3170929>

**Important note**

To cite this publication, please use the final published version (if applicable).  
Please check the document version above.

**Copyright**

Other than for strictly personal use, it is not permitted to download, forward or distribute the text or part of it, without the consent of the author(s) and/or copyright holder(s), unless the work is under an open content license such as Creative Commons.

**Takedown policy**

Please contact us and provide details if you believe this document breaches copyrights.  
We will remove access to the work immediately and investigate your claim.

***Green Open Access added to TU Delft Institutional Repository***

***'You share, we take care!' - Taverne project***

**<https://www.openaccess.nl/en/you-share-we-take-care>**

Otherwise as indicated in the copyright section: the publisher is the copyright holder of this work and the author uses the Dutch legislation to make this work public.

# A 76.5–92.6 GHz CMOS LNA Using Two-Port $kQ$ -Product Theory for Transformer Design

Youming Zhang<sup>ID</sup>, Member, IEEE, Zhennan Wei<sup>ID</sup>, Xusheng Tang<sup>ID</sup>, Linghan Zhang,  
and Fengyi Huang<sup>ID</sup>, Member, IEEE

**Abstract**—This letter presents a convenient approach based on the two-port  $kQ$ -product theory to analyze the influence of interwinding capacitive coupling on the efficiency of the transformer. It is demonstrated that a transformer with proper size can benefit from the interwinding capacitive coupling to maximize its efficiency at a desired frequency. The proposed design approach is used in a  $W$ -band low-noise amplifier (LNA) fabricated with the 40-nm CMOS process to optimize the insertion loss of the input transformer-based balun. Thanks to the approach, the  $W$ -band LNA achieves a minimum noise figure of 5.7 dB, a maximum gain of 18.5 dB, and a 3-dB bandwidth of 76.5–92.6 GHz, while consuming 23.4 mW from a 0.9-V supply.

**Index Terms**— $kQ$ -product, low-noise amplifier, millimeter-wave (mmWave), transformer,  $W$ -band.

## I. INTRODUCTION

RECENTLY there has been an emerging demand for millimeter-wave (mmWave) integrated circuits for wireless communication and radar applications such as the  $E$ -band high data rate communication and the 77-GHz/79-GHz/90-GHz radar. As the first block in a receiver, the low-noise amplifier (LNA) plays a critical role in the performance of the whole system. LNA is required to provide sufficient gain with a low noise figure (NF) to improve the receiver's sensitivity.

In the LNA design, the differential configuration is usually preferred due to its immunity to common-mode noise from the ground and supply. In this case, an input balun, which is mostly made by an on-chip transformer in mmWave circuits, is needed for single-end-to-differential conversion. However, as the first stage, the transformer-based input balun contributes a significant part to the LNA's NF. Hence, it is important to design a transformer with low insertion loss (IL) and high efficiency to minimize its NF degradation to LNA.

Several efforts have been made to elaborate the transformer's efficiency at mmWave frequencies. Zhao and Reynaert [1] show by simulation that transformers with larger

size tend to exhibit higher maximum efficiency (or lower IL) due to larger magnetic coupling between the two windings. As an improvement, the formula of transformers' maximum efficiency  $\eta_{\max}$  was declared in [2]. It shows that the maximum efficiency is positively related to the product of the coupling coefficient  $k$  and the quality factor  $Q$  of the winding. In fact, as early as 2007, Kurs *et al.* [3] revealed that not  $k$  alone but the  $kQ$ -product plays a pivotal role in coupled resonant coils [3]. Then, the  $kQ$ -product theory has become a powerful tool and actually been extended to represent general two-port systems' transfer characteristics [4], [5].

However, articles no matter about circuit design or two-port system analysis generally did not consider the nonignorable capacitive coupling between the two windings of a transformer to facilitate transformers' maximum efficiency. Intuitively, the interwinding capacitive coupling creates a new path for power transmission, and thus it is possible to be used to enhance the efficiency of the transformer. So far, a thorough design methodology about interwinding capacitive coupling effect for maximizing on-chip transformer efficiency is still lacking.

Therefore, in this letter, we present an approach based on the two-port  $kQ$ -product theory to analyze the effects of capacitive coupling in an on-chip transformer, so as to provide a more convenient way to facilitate efficiency optimization of the on-chip transformer. To validate it, a  $W$ -band LNA is designed with transformer-based input balun implemented in the 40-nm CMOS process. The LNA achieves competitive overall performances with a minimum NF of 5.7 dB at 91 GHz, a maximum gain of 18.5 dB, a 3-dB BW of 76.5–92.6 GHz, and a compact chip area.

## II. TRANSFORMER EFFICIENCY OPTIMIZATION DESIGN BASED ON $kQ$ -PRODUCT THEORY

To analyze the effects of interwinding capacitive coupling on the maximum efficiency ( $\eta_{\max} = 10^{G_{\max}/10}$ ) of a transformer, the two-port  $kQ$ -product theory has been introduced in this letter. In [5], the definition of  $kQ$ -product is extended as a general metric for the power transfer potentiality of all two-port systems. The larger  $kQ$ -product that a two-port system has, the higher  $\eta_{\max}$  will be achieved. The definition of  $kQ$ -product in [5] is expressed as below:

$$kQ = |Z_{21}|/\text{ESR}. \quad (1)$$

In this equation, ESR is called the *equivalent scalar resistance* of a two-port system and indicates the system's loss assessment in the immittance domain [5]. It is formulated as

$$\text{ESR} = \sqrt{\text{Re}[Z_{11}]\text{Re}[Z_{22}] - \text{Re}[Z_{12}]\text{Re}[Z_{21}]}. \quad (2)$$

Manuscript received 19 March 2022; accepted 24 April 2022. Date of publication 5 May 2022; date of current version 7 October 2022. (Corresponding author: Youming Zhang.)

Youming Zhang, Xusheng Tang, and Fengyi Huang are with the School of Cyber Science and Engineering, School of Microelectronics, Southeast University, Nanjing 210096, China, and also with the Purple Mountain Laboratories, Nanjing 211111, China (e-mail: zhangyouming@seu.edu.cn).

Zhennan Wei is with the School of Information Science and Engineering, Southeast University, Nanjing 210096, China.

Linghan Zhang was with the School of Information Science and Engineering, Southeast University, Nanjing 210096, China. He is now with the Department of Microelectronics, Technische Universiteit Delft, 2628 Delft, The Netherlands.

Color versions of one or more figures in this letter are available at <https://doi.org/10.1109/LMWC.2022.3170929>.

Digital Object Identifier 10.1109/LMWC.2022.3170929

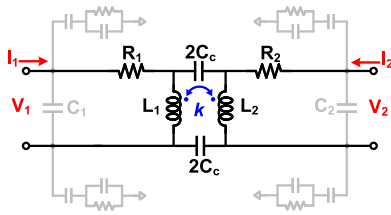


Fig. 1. Simplified equivalent circuit model of the transformer.

The simplified equivalent circuit model of the transformer is shown in Fig. 1. In this model, the interwinding capacitive coupling effect is modeled as two capacitors ( $C_c$ ) between the primary and secondary windings. For simplicity, the substrate parasitic elements are neglected, and symmetry assumption is made to this model, namely,  $L_1 = L_2 = L$  and  $R_1 = R_2 = R$ . In addition, because shunt capacitance  $C_1$  and  $C_2$  can be absorbed into the forward and rear matching networks, they will not be included in the  $kQ$ -product equation. Thus, we can obtain

$$Z_{11} = Z_{22} = R + j\omega L \frac{-\omega^2(1-k^2)LC_c}{1-2\omega^2(1-k)LC_c} \quad (3)$$

$$Z_{12} = Z_{21} = j\omega L \frac{k - \omega^2(1-k^2)LC_c}{1-2\omega^2(1-k)LC_c}. \quad (4)$$

Then, the  $kQ$ -product of the transformer can be expressed as

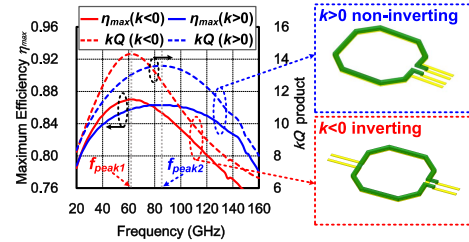
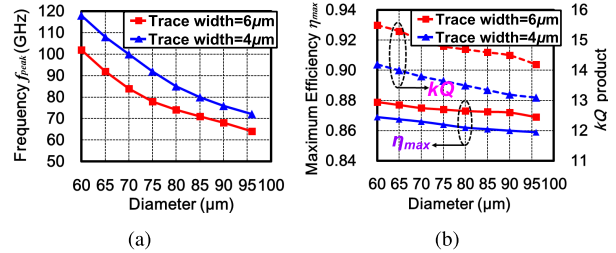
$$kQ = \frac{\omega L}{R} \left| \frac{k - \omega^2(1-k^2)LC_c}{1-2\omega^2(1-k)LC_c} \right|. \quad (5)$$

Since  $\omega L/R$  is the  $Q$ -factor of the windings, it can be obviously found that if  $C_c$  is neglected, the right side of (5) will become  $(\omega L/R)k$  and less than the  $Q$ -factor of the windings. However, when  $C_c$  is considered, the equivalent coupling effects of the transformer are boosted and the  $kQ$ -product exhibits a maximum value at

$$f_{\text{peak}} = \frac{1}{2\pi\sqrt{2(1-k)LC_c}} \quad (6)$$

which means that a peak  $\eta_{\text{max}}$  can be achieved at  $f_{\text{peak}}$ . It just reflects that interwinding capacitive coupling is potential to boost the efficiency of the transformer at appropriate operating frequency band. Note that although the right side of (5) approximates to infinity at  $f_{\text{peak}}$ , due to the substrate loss and the effects from other high-order parasitic elements, the peak  $kQ$ -product at  $f_{\text{peak}}$  of a real transformer will actually be a finite value.

To validate the above analysis approach, two on-chip transformers are inserted into electro-magnetic (EM) simulator, and the  $kQ$ -product and  $\eta_{\text{max}}$  are shown in Fig. 2. The two transformers have the same diameter and trace width but different signs of  $k$ -factor. It can be seen that the curves of the  $kQ$ -product and  $\eta_{\text{max}}$  of the transformer have the same peak frequency and trend. The inverting ( $k < 0$ ) and noninverting ( $k > 0$ ) transformers exhibit peak  $kQ$ -product and  $\eta_{\text{max}}$  at  $f_{\text{peak1}}$  and  $f_{\text{peak2}}$ , respectively, while the inverting transformer has a lower  $f_{\text{peak}}$  than its noninverting counterpart, which can also be derived from the equation of  $f_{\text{peak}}$ . Thus, the

Fig. 2. Simulated  $kQ$ -product and  $\eta_{\text{max}}$  of transformers.Fig. 3. Simulated (a)  $f_{\text{peak}}$  and (b)  $\eta_{\text{max}}$  and  $kQ$ -product versus diameters under different trace widths of the one-coil transformers with stacked top two thick metal layers.

$kQ$ -product is able to be used to characterize the power transfer potentiality of on-chip transformers.

As shown in (5) and (6), the  $kQ$ -product (or  $\eta_{\text{max}}$ ) of a transformer can be maximized at  $f_{\text{peak}}$  by choosing proper winding inductance  $L$ ,  $k$  and interwinding capacitance  $C_c$ . Since parameters  $L$ ,  $k$ , and  $C_c$  are closely related to the sizing parameters of a transformer, geometrical size such as the diameter and trace width needs to be properly designed.

For the  $W$ -band application, the top two thick metal layers are used to construct stacked one-coil transformer to reduce the parasitic resistance and the substrate parasitic effect resulting in enhanced  $kQ$ -product. The  $f_{\text{peak}}$  for the trace width varying from 4 to 6  $\mu\text{m}$  and the diameter in the range of 60–100  $\mu\text{m}$  are plotted in Fig. 3(a). The corresponding  $kQ$ -product and  $\eta_{\text{max}}$  are plotted in Fig. 3(b). We can easily pick and choose the transformer with diameter of 75  $\mu\text{m}$  and trace width of 6  $\mu\text{m}$  that achieves a  $f_{\text{peak}}$  of roughly 80 GHz and a  $\eta_{\text{max}}$  of 0.87, which translates to a minimum IL of only 0.6 dB.

### III. $W$ -BAND LNA DESIGN

Fig. 4 shows the schematic of the proposed  $W$ -band LNA with important device parameters. LNA consists of three stages of pseudo-differential common-source amplifiers. The capacitive neutralization technique is adopted in the second and third stages to improve LNA's gain and stability. The input matching network is implemented with a transformer-based balun in series with transmission lines (TLs) for broadband matching.

The proposed transformer design approach based on the two-port  $kQ$ -product theory is used to minimize the IL of the transformer. In the transformer design, the stack structure is chosen to realize proper interwinding capacitance to obtain the peak  $\eta_{\text{max}}$  at the desired frequency.

Since interwinding capacitance of the transformer-based balun can lead to differential imbalance, bypass capacitance CB is implemented with metal-oxide-metal (MOM) capacitors to short the center tap to ac ground to mitigate the imbalance, and with custom-designed MOS capacitors to enhance

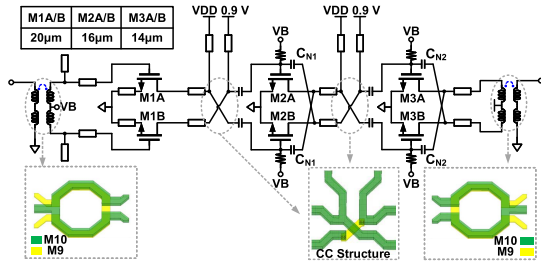


Fig. 4. Schematic of the proposed LNA.

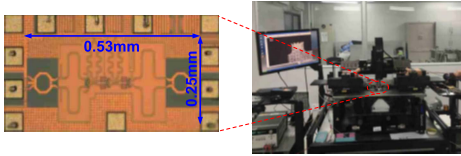


Fig. 5. Measurement setup and chip micrograph of the proposed LNA.

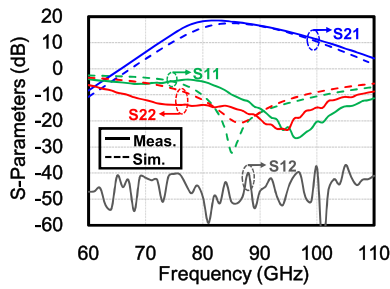


Fig. 6. Measured and simulated  $S$ -parameters of the proposed LNA.

stability of LNA. The cross-coupling (CC) structures are used to mitigate the asymmetry introduced by interstage TLs.

To further improve LNA’s gain and NF performance, the bottom two metal layers ( $M1$  and  $M2$ ) are stacked together to make the ground plane of the microstrip lines, which reduces the ohmic loss in the ground plane. Simulation shows that compared with single metal later ( $M1$ ),  $M1$  and  $M2$  stacking structure can improve the gain and NF of LNA by 0.9 and 0.4 dB, respectively.

IV. IMPLEMENTATION AND MEASUREMENT

The  $W$ -band LNA is implemented in the 40-nm CMOS technology. Fig. 5 shows the measurement setup and the chip micrograph. The LNA occupies a core chip area of  $0.53 \times 0.25 \text{ mm}^2$  and consumes 23.4 mW from a 0.9-V supply. On-wafer  $S$ -parameter measurement is shown in Fig. 6. The maximum  $S_{21}$  is 18.5 dB at 84 GHz with a 3-dB BW of 76.5–92.6 GHz. The discrepancy between the measurement and simulation results mainly attributes to modeling inaccuracies in EM simulation. Rollett stability factor  $K_f$  and  $\Delta$  are shown in Fig. 7(a) indicating unconditional stable. A simulated  $IP1$  dB of above  $-19$  dBm is achieved and shown in Fig. 7(b). A 75–110-GHz noise source and a Keysight N8975A NF analyzer are used to measure NF in Fig. 8. A  $W$ -band preamplifier is used following LNA to provide enough gain to improve the system noise floor. IL of ground-signal-ground (GSG) probes and noise of the preamplifier can be calibrated out. The measured NF ranges from 5.7 to 7.3 dB in the 3-dB BW with a minimum value of 5.7 dB at 91 GHz.

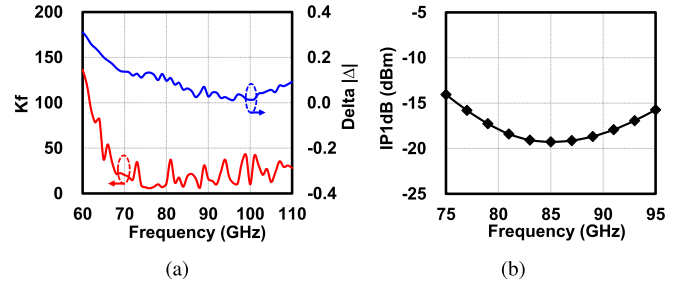


Fig. 7. (a) Measured stability factor  $K_f$  and  $\Delta$ . (b) Simulated  $IP1$  dB.

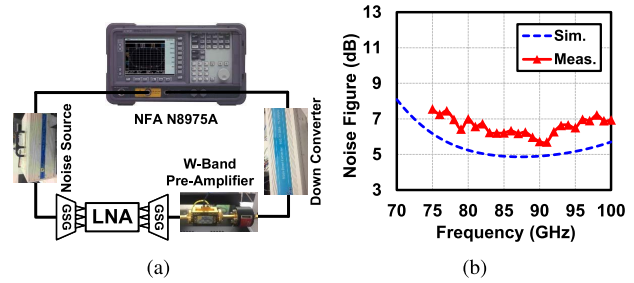


Fig. 8. (a) NF measurement setup. (b) Measured and simulated NF.

TABLE I  
COMPARISON WITH PRESENTED CMOS MMWAVE LNAs

Ref.	This Work	[6] MWCL'16	[7] JSSC'17	[8] TMTT'20	[9] IMS'20		
Process (nm)	40-nm CMOS	65-nm CMOS	65-nm CMOS	22-nm FD-SOI	55-nm CMOS		
$f_0$ (GHz)	84	104	77.25	77	92		
BW (GHz)	16.1	21.5	27.5	30	13	31	7.6*
Gain (dB)	18.5	16.7	13.3	18.5	24	18.2	15
NF (dB)	5.7–7.3	7.2–9.0	6.4–8.5	5.5–7.9	4.6#	5.8–7.5#	5.0–7.5
Supply (V)	0.9	1.8	1.2	1.8	1.6	1.6	1.2 & 2.0
Power (mW)	23.4	45	12	27	16	16	72.7
Area ( $\text{mm}^2$ )	0.174	0.29	0.24	0.35	0.43	0.106	
FoM* (dB)	2.5–6.6	-6.5–-2.3	4.8–10.0	5.1–11.3	16.7	10.6–15.0	-17.9–-11.3

\* 5-dB BW is 23.5 GHz.

# 4.6dB is the Minimum NF, and 5.8–7.5 dB is partial frequency band (90–96 GHz) NF.

\*  $FoM = 20 \log_{10} \left( \frac{Gain[\text{lin.}] \cdot BW[\text{GHz}]}{P_{dc}[\text{mW}] \cdot (NF[\text{lin.}] - 1)} \right)$

The measured results are summarized and compared with the prior arts [6]–[9] in Table I. Thanks to the proposed approach using two-port  $kQ$ -product theory for transformer design, the  $W$ -band LNA in this letter exhibits competitive overall performances with an excellent NF under low supply voltage and compact chip area.

V. CONCLUSION

This letter presents a convenient approach to evaluate and optimized the effects of interwinding capacitive coupling on a transformer. By properly designing the winding inductances,  $k$ -factor, and interwinding capacitances, the efficiency of the transformer can be maximized at the desired frequency. This design approach is then validated in a  $W$ -band CMOS LNA as to optimize the transformer-based balun. Under a low supply voltage of 0.9 V, LNA presents good overall performances with a measured NF of 5.7–7.3 dB, a maximum gain of 18.5 dB, a 3-dB BW of 76.5–92.6 GHz, and a 23.4-mW power consumption, as well as a compact chip area.

## REFERENCES

- [1] D. Zhao and P. Reynaert, "A 60-GHz dual-mode class AB power amplifier in 40-nm CMOS," *IEEE J. Solid-State Circuits*, vol. 48, no. 10, pp. 2323–2337, Oct. 2013.
- [2] W. Shin, S. Callender, S. Pellerano, and C. Hull, "A compact 75 GHz LNA with 20 dB gain and 4 dB noise figure in 22 nm FinFET CMOS technology," in *Proc. IEEE Radio Freq. Integr. Circuits Symp. (RFIC)*, Jun. 2018, pp. 284–287.
- [3] A. Kurs, A. Karalis, R. Moffatt, J. D. Joannopoulos, P. Fisher, and M. Soljačić, "Wireless power transfer via strongly coupled magnetic resonances," *Science*, vol. 317, no. 5834, pp. 83–86, 2007.
- [4] T. Ohira, "What in the world is Q?" *IEEE Microw. Mag.*, vol. 17, no. 6, pp. 42–49, Jun. 2016.
- [5] T. Ohira, "The kQ product as viewed by an analog circuit engineer," *IEEE Circuits Syst. Mag.*, vol. 17, no. 1, pp. 27–32, 4th Quart., 2017.
- [6] G. Feng, C. C. Boon, F. Meng, X. Yi, and C. Li, "An 88.5–110 GHz CMOS low-noise amplifier for millimeter-wave imaging applications," *IEEE Microw. Wireless Compon. Lett.*, vol. 26, no. 2, pp. 134–136, Feb. 2016.
- [7] G. Feng *et al.*, "Pole-converging intrastage bandwidth extension technique for wideband amplifiers," *IEEE J. Solid-State Circuits*, vol. 52, no. 3, pp. 769–780, Mar. 2017.
- [8] L. Gao, E. Wagner, and G. M. Rebeiz, "Design of E- and W-band low-noise amplifiers in 22-nm CMOS FD-SOI," *IEEE Trans. Microw. Theory Techn.*, vol. 68, no. 1, pp. 132–143, Jan. 2020.
- [9] K. Zhang, C. Shi, G. Chen, J. Chen, and R. Zhang, "A 64.5–88 GHz coupling-concerned CMOS LNA with >10 dB gain and 5 dB minimum NF," in *IEEE MTT-S Int. Microw. Symp. Dig.*, Aug. 2020, pp. 337–340.